JCTC Journal of Chemical Theory and Computation

ARTICLE

pubs.acs.org/JCTC

Microsolvation Effect on the Twist of β-sheets

Joel Ireta*

Departamento de Química, División de Ciencias Básicas e Ingeniería, Universidad Autónoma Metropolitana-Iztapalapa, A.P. 55-534, México D. F. 09340

ABSTRACT: Under certain circumstances β-sheets prefer to be twisted instead of flat. To get insight into the reasons of such preference, bare and microsolvated parallel and antiparallel two-strand polyalanine β-sheets are investigated using density functional theory. Full geometry optimizations show that microsolvation increases interstrand twisting and promotes a flat to twist transition. It is found that the latter behavior is connected to compressive strain resulting from microsolvation. Residues in flat β-sheets adjust the sense of its local intrastrand twist, which leads to the appearance of interstrand twist, to release strain and to favor water−water hydrogen bonding. The predicted microsolvation effect is corroborated analyzing the geometry of residues forming β-sheet motifs in protein crystals.

1. INTRODUCTION

β-sheets are characteristic structural motifs of proteins and polypeptides. Such motifs consist of two or more parallel or antiparallel hydrogen-bonded peptide strands.[1] There is a renewed interest in studying β-sheets since it was discovered that its aggregation plays a central role in the mechanism underlying several diseases, including alzheimer's, Huntington's, Parkinson's, and the prion encephalopathies.[2−6] A large number of theoretical studies have been devoted to investigate formation, stability, and geometric peculiarities of β-sheets.[7−17] Nevertheless basic questions regarding their structure are still open. For example, polypeptides, like polyalanine, segments from proteins that form amyloid-like fibrils, fibrous proteins, like silk and β-keratin, crystallize as flat β-sheets, i.e., the chain axes of the strands forming the sheet lay on the same plane. β-sheet motifs in globular protein crystals, however, show large and systematic structural deviations with respect to the classical (flat) geometry.[18−20] They show an interstrand right-handed twist coupled to an intrastrand left-handed twist,[18] i.e., chain axes are not coplanar, and strand peptide units are converted into the next along the backbone by a rotation that systematically differs from 180°. There is no consensus on the causes that originate the twist of β-sheets. It has been proposed that the twist is either intrinsic to isolated strands or induced by interchain interactions. The emergence of the twist as an intrinsic feature of isolate β-strands has been suggested to be connected to entropic factors that lower the free energy of left-hand twisted chains with respect to straight or right-handed ones,[18] to the tendency of the backbone C−C single bond to eclipse the lone pair of the backbone N atom,[12] to the electrostatic attraction between the carbonyl carbon of one peptide unit and the carbonyl oxygen of an adjacent peptide unit,[7] and to intrastrand steric hindrances between the oxygen of the carbonyl group and the side chain.[20,8] The emergence of the twist as a consequence of interstrand interactions has been attributed to constraints imposed by hydrogen-bond (hb) formation,[9] to intra- and interstrands interactions involving side groups[10] and to interstrand electrostatic interactions.[11] Recently it was found that segments from proteins forming amyloid-like fibrils crystallize as flat sheets.[2,3] Studies using molecular dynamics simulations and empirical force fields, however, reported that these systems tend to twist in solution,[21,22] suggesting that β-sheets twist as a response to external conditions and that β-sheets adopt both flat and twisted conformations. Theoretical studies considering the full role of the self-consistent electronic structure and a full optimization of the geometry have found that both twisted and flat conformations are stable structures and that the energy related to twisting is negligible.[13] Other study based on electronic structure calculations found that breaking side chain−backbone hbs promotes the formation of a twisted β-sheet.[23] In this work the origin of twisting is investigated by constructing atomistic models for flat and twisted two-strand parallel and antiparallel polyalanine β-sheets. Their geometries were fully optimized using density functional theory (DFT). The influence of hydration on twisting is investigated microsolvating the models with explicit water molecules and fully optimizing their geometries. Moreover, hydration effect on twisting is also investigated analyzing preferred conformations of residues in contact with water molecules in β-sheet motifs in protein crystal structures.

As detailed below, it was found that both twisted and flat structures are intrinsic conformations of two-strand antiparallel and parallel polyalanine β-sheets in vacuum. It is shown that strands in all the structures are under compressive strain, owing primarily to interstrand hydrogen bonding. The backbone response to strain provokes local intrastrand twisting along the strands. Nevertheless flat β-sheets in vacuum did not develop noticeable interstrand twisting because residues locally twist in both senses. It was also found that flat β-sheets transform to twisted ones upon hydration. The latter behavior is connected to further compressive strain resulting from microsolvation. Residues in flat β-sheets adjust the sense of its local intrastrand twist, which leads to the appearance of interstrand twist, to release strain and to favor water−water hydrogen bonding. Furthermore comparing average geometries of residues (except glycine and proline) forming β-sheet motifs in protein crystals, it is corroborated the predicted effect of hydration on the twist of β-sheets.

Received: March 29, 2011
Published: June 30, 2011

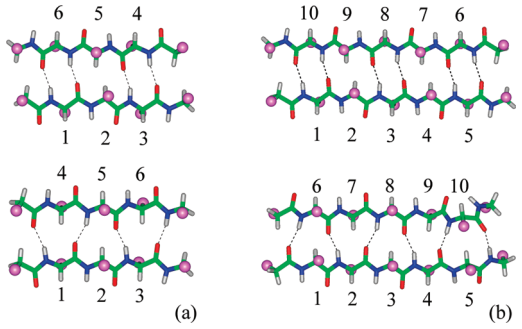

Figure 1. (a) Short polyalanine β-sheet models constructed with three residues per strand: upper structure, antiparallel β-sheet model and lower structure, parallel β-sheet model. Residue labels go from 1 to 6. (b) Large polyalanine β-sheet models constructed with five residues per strand: upper structure, antiparallel β-sheet model and lower structure, parallel β-sheet model. Residue labels go from 1 to 10. Nitrogen atoms are in blue, carbon atoms in green, oxygen atoms in red, and hydrogen atoms in light gray. For clarity methyl groups are represented as pale magenta balls. Dotted lines indicate hbs.

The latter result also suggests that the peptide aminoacid composition (excluding glycine and proline) does not determine if a β-sheet adopts a flat or a twisted conformation.

2. METHOD

Full geometry optimizations were carried out using DFT together with the generalized gradient approximation of Perdew, Burke, and Ernzerhof (PBE) for the exchange−correlation functional.[24] Conformations of the structures here investigated are primarily dictated by the formation of hbs, and such hbs are described by DFT using PBE (thereafter called DFT-PBE) within an error of 1 kcal/mol with respect to Møller−Plesset second-order perturbation theory (MP2) results.[25] It has been shown that geometric parameters obtained with DFT-PBE for an extensive set of hydrogen-bonded dimers, including dimers formed with peptide-like molecules, are in good agreement with those obtained with MP2, except for cases in which hbs in the dimer are highly bent.[25] In the full optimized β-sheet models intrastrand hbs are close to linearity, the largest deviation found for the N−H···O angle is of 25° with respect to linearity (i.e., respect to 180°). This gives us confidence on the DFT-PBE geometries obtained here. DFT-PBE does not describe van der Waals interactions properly. However it is expected minimal alteration of the energy trends obtained here as the spatial distribution of atoms around a given one in flat and twisted conformations is very similar. Troullier−Martins pseudopotentials,[26,27] plane-wave basis sets, and periodic boundary conditions are used for solving the DFT Kohn−Sham equations as it is incorporated in the abinit code.[28,29] Here it is worth noting that the use of plane waves does not introduce a basis set superposition error.[25] Eight structural models consisting of two strands were constructed for investigating favorable β-sheet conformations. Four models were constructed in a parallel β-sheet conformation and four in an antiparallel β-sheet conformation. These models differ in their number of residues per strand. The thereafter called short models (Figure 1a) were built with three residues per strand, and those built with five residues per strand are called large models (Figure 1b). Structures called flat were built as flat β-sheets, and structures called twisted were built as twisted β-sheets. Antiparallel short β-sheets are labeled as structures I (flat) and II (twisted). Parallel short β-sheets are labeled as structures III (flat) and IV (twisted). Antiparallel large β-sheets are labeled as structures V (flat) and VI (twisted). Finally parallel large β-sheets are labeled as structures VII (flat) and VIII (twisted). Strands were capped with the CH_3CH_2CO- group in the N terminus and with the CH_3CH_2NH- group in the C terminus. As periodic boundary conditions were used for solving the DFT Kohn−Sham equations, the calculations were carried out using a supercell sufficiently large enough to ensure that interactions with the periodic images were negligible. Here an orthorhombic supercell was used to fully optimize the geometry. For all the calculations the energy cutoff of the plane wave basis set was 70 Ry, and the sampling of the Brillouin zone was replaced by the Γ-point.

Conformations of residues are given here in terms of local cylindrical coordinates instead of the standard ϕ and ψ coordinates. The latter is found convenient because cylindrical coordinates give a direct measurement of intrastrand twisting, while using dihedral angles only an approximate estimation can be done for twisting. However, the procedure to determine cylindrical coordinates is rather involved, and it is explained next. The relative position of the i-th residue respect to its neighbors along the polypeptide chain is given in terms of a certain rotation θ_i (the twist) and a certain translation L_i (the rise) along a local chain axis $\mathbf{z}_i$. These parameters define a screw symmetry operation that superimposes the coordinates of the peptide bonds flanking the α-carbon of the i-th residue. For left-handed rotations θ is defined to be $\theta > 180°$. Here is more convenient to report the degree of local intrastrand twist as $\tau_i = \theta_i - 180°$, thus $\tau > 0$ for left-handed intrastrand twist. The local interstrand twist, T_{ij}, is calculated as the smallest angle formed between the local chain axis vectors $\mathbf{z}_i$ and $\mathbf{z}_j$. These vectors are connected to the i- and j-th interstrand hydrogen-bonded residues in the β-sheet. For right-handed interstrand twist T_{ij} is defined to be $T_{ij} > 0$. The quaternion-based superposition fit method[30−33] is used to determine the cylindrical coordinates θ_i, L_i, and $\mathbf{z}_i$ for each residue. In this method θ and L are such that minimize the root-mean-square deviation of distances between the set of superimposed coordinates (for further details see, e.g., ref 33). It has been shown that the use of cylindrical coordinates is advantageous for mapping the conformational space of residues in finite and infinite polypeptides as well as in protein structures.[33−36]

For building the initial structure of the strands forming the β-sheet models, the equilibrium geometry of a residue in an infinitely long polyalanine chain is used. For flat sheets, the corresponding geometry of a residue in a fully extended structure (FES, with $\phi = -159.7°$ and $\psi = 164.4°$), in which $L = 3.57$ Å and $\theta = 180°$ ($\tau = 0°$) is used.[35] As compressed polyalanine FES develop a left-handed twist (see Figure 3b in ref 33), for twisted sheets the geometry used for each residue corresponds to that in a compressed FES (with $\phi = -120.4°$ and $\psi = 150.4°$), in which $L = 3.39$ Å and $\theta = 196.4°$ ($\tau = 16.4°$). This local left-handed intrastrand twist forces to build the β-sheet with an interstrand right-handed twist to keep reasonable interstrand hb distances. To estimate the influence of hydration on the relative stability and the structure of twisted and flat conformations, the short-antiparallel β-sheet models are microsolvated with explicit water molecules. Hydrated β-sheet models were built using 8, 16, and 20 water molecules, half of them for microsolvating one strand and the rest for microsolvating the other one. Certainly there are many ways water molecules self-arrange around peptide strands, for example, forming water clusters at certain positions along the

Table 1. Local Geometry Parameters (L_i, τ_i) for Residues in Short β-Sheet Structures I−IV

	I		II		III		IV	
residue label	L	τ	L	τ	L	τ	L	τ
1	3.53	8.9	3.47	24.3	3.47	2.4	3.47	1.1
2	3.52	2.2	3.49	8.3	3.45	0.2	3.42	19.1
3	3.52	−7.9	3.43	−7.2	3.41	4.9	3.42	9.6
4	3.51	11.2	3.46	23.9	3.46	9.5	3.37	36.4
5	3.51	3.6	3.50	8.7	3.44	1.6	3.43	−0.4
6	3.50	−8.1	3.45	−5.6	3.43	−3.6	3.35	5.0

strands, and some of them may be lower in energy than the arrangements investigated here. A full exploration of the conformational space of such microsolvated systems is out of the scope of this work. Here, water molecules were adsorbed such that they formed hbs with the −N−H amide groups and the −C═O carbonyl groups that were not interstrand hydrogen bonded. The rest of water molecules, if any, were absorbed such that an uninterrupted network of hbs was formed along the water molecules. The purpose of the latter is to investigate the effect of water−water hb cooperativity on the twist of the β-sheets. It is expected that hydrated models constructed in such way resemble better a fully solvated peptide. Full geometry optimizations of each of the microsolvated models were carried out using DFT-PBE.

Preferred conformations that residues adopt in β-sheet motifs in proteins are investigated by analyzing an extended set of protein structures resolved by X-ray crystallography and obtained from the protein data bank (PDB).[37] The set of 1591 structures was formed with protein structures determined at 1.5 Å resolution or better and a sequence identity of less than 50%. It was corroborated that the result of the analysis is independent from the X-ray resolution and the percentage of sequence identity. The set of analyzed residues does not contain glycines and prolines, as the conformational space of these two residues is known to be markedly different from others, owing to the lack of a side group in glycine and the constraints imposed by the ring formation in the proline backbone. Residues flanking glycines and prolines were also excluded from the analyzed set. A residue was considered to be part of a β-sheet motif if it was in an extended conformation, i.e., if $L > 2.8$ Å[33] and if peptide bonds flanking its α-carbon were hydrogen bonded to peptide bonds flanking the α-carbon of a residue also in an extended conformation and separated at least three positions along the chain. Two peptide bonds were considered to be hydrogen bonded if the distance between the O atom (hb acceptor atom) and the N atom (hb donor atom) was smaller than 3.3 Å and the angle C═O···N bigger than 120°. It was corroborated that the main characteristics of the distributions for L, τ, and T thus obtained were not dependent on the latter two parameters. A residue was taken into account for the analysis only if it belonged to a part of the structure where at least three consecutive residues were found in a β-sheet conformation. In this way ending effects and β-bridges were avoided.

3. RESULTS

Let me first discuss the fully optimized geometries for the bare flat and twisted short β-sheet models. The values for the local geometric parameters (L_i, τ_i) are given in Table 1. First, it is noticeable that all L values are smaller than $L_{FES} = 3.57$ Å (the rise of a residue in FES), indicating that all residues in structures I−IV are under compressive strain. Recalling that the geometry of an optimized isolated strand is the FES, a residue under compressive strain is then characterized by $L < L_{FES}$, i.e., its length is shorter than the corresponding one in the FES. Likely, such compressive strain is originated by interstrand hydrogen bonding, i.e., longer hbs than the observed ones are expected if strand compression is not allowed. All residues present some degree of intrastrand twist, i.e., τ significantly deviates from zero. Residues at the end of each strand (those labeled with numbers 1, 3, 4, and 6 in Figure 1a) tend to be more twisted and more compressed than the central residue. To avoid ending effects on the structural trends, only central residues are considered for analysis. The average values of τ for the central residue in structures I and III, the flat antiparallel and parallel short β-sheet models, are 2.9° and 0.9°, respectively. However the corresponding average values of τ for the central residue in structures II and IV, the twisted antiparallel and parallel short β-sheet models, are 8.5° and 9.3° respectively, i.e., intrastrand left-handed twist is at least three times larger in the fully relaxed twisted models than in the fully relaxed flat models. Local interstrand twist values, T_{ij}, are listed in Table 2. According to these values all residues present some degree of interstrand twist, however, focusing only on central residues T values indicates that structures I and III are flat, i.e., $T < 1°$, but structures II and IV are significantly twisted, $T > 11°$. Side views of the fully relaxed structures I to IV are shown in Figure 2a. There is evidence that fully relaxed structures II and IV present interstrand twist, however, fully relaxed structures I and III are flat, as indicated by the T values corresponding to their central residues.

Table 2. $T_{i,j}$ Values for Residues in Short β-Sheet Structures I−IV

residue labels	I	II	residue labels	III	IV
1, 6	−6.5	13.8	1, 4	−5.7	21.3
2, 5	0.9	11.1	2, 5	−0.2	15.9
3, 4	6.0	14.8	3, 6	4.9	13.9

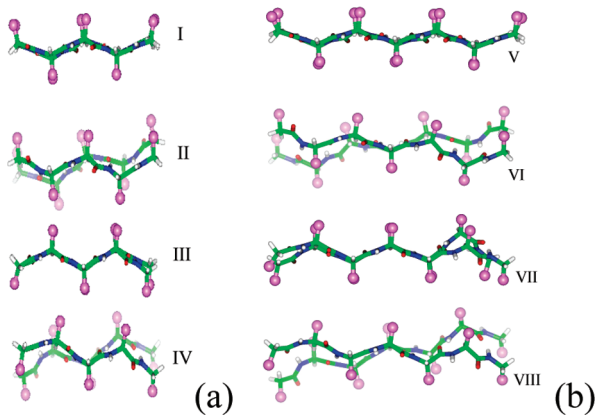

Figure 2. Side view of the fully relaxed geometries for the (a) short and (b) large polyalanine β-sheet models. For the color code see caption of Figure 1. For clarity methyl groups are represented as pale magenta balls.

Table 3. Local Geometry Parameters (L_i, τ_i) for Residues in Large β-Sheet Structures V−VIII

	V		VI		VII		VIII	
residue label	L	τ	L	τ	L	τ	L	τ
1	3.51	11.4	3.4	30.1	3.48	3.35	3.48	3.0
2	3.53	1.1	3.5	9.6	3.42	0.1	3.46	15.6
3	3.55	−1.0	3.54	7.6	3.45	8.1	3.45	7.9
4	3.52	0.6	3.46	12.4	3.5	12.3	3.44	18.2
5	3.49	−8.4	3.36	−6.6	3.49	7.68	3.45	10.5
6	3.51	12.7	3.43	31.3	3.39	20.61	3.35	39.5
7	3.53	2.8	3.5	10.2	3.47	3.3	3.48	3.0
8	3.54	−1.4	3.55	6.3	3.48	−5.0	3.5	9.8
9	3.52	2.1	3.49	9.3	3.29	−9.7	3.43	4.2
10	3.48	−10.8	3.39	−4.3	2.88	1.75	3.27	7.7

Table 4. $T_{i,j}$ Values for Residues in Large β-Sheet Structures V−VIII

residue labels	V	VI	residue labels	VII	VIII
1, 10	−8.6	18.4	1, 6	10.1	21.3
2, 9	−1.0	14.4	2, 7	3.5	14.3
3, 8	−0.4	12.7	3, 8	3.6	16.0
4, 7	1.6	14.7	4, 9	17.2	20.0
5, 6	7.6	19.0	5, 10	6.1	14.1

To verify independence of intra- and interstrand twist with respect to strand length, four polyalanine β-sheet models built using five residues per strand (the large models) were also fully optimized using DFT-PBE. The corresponding values for the local geometric parameters (L_i, τ_i) are listed in Table 3. As for the short models, L values indicate that all residues are under compressive strain. Also all residues present some degree of intrastrand twist, and those at strand endings (residues labeled with the numbers 1, 5, 6, and 10) are more compressed and more twisted than those in the middle of the strands. Focusing on central residues, labeled with the numbers 2−4 and 7−9 in Figure 1b, it is found that intrastrand twist is significantly smaller for structures V and VII than for structures VI and VIII. Average values for τ in structures V and VII, the flat large models, are 0.7° and 1.5°, respectively. However, average values for τ in structures VI and VIII, the twisted large models, are 9.2° and 9.8°, respectively, i.e., the fully relaxed twisted large models present an intrastrand twist at least six times larger than the fully relaxed flat large models. Local interstrand twist values, T_{ij}, for the large models are listed in Table 4. Average values (considering only central residues) for T are 0.1° and 8.1° for structures V and VII, respectively. The average T value for structure VII is significantly larger than the average T value for structure V, owing to a large local interstrand twist in residues close to the right end of the sheet. Such distortion is due to the formation of an intrastrand hb between residues 9 and 10 in structure VII. Still interstrand twisting is not noticeable in such structures (Figure 2b). In the short flat parallel β-sheet, model III, an intrastrand hb similar to that in model VII is not formed. Likely the potential energy surface associate to strand endings is quite flat, small fluctuations in the forces may thus drive strand endings to conformations noticeably different among the models. This may be also the reason for the discrepancy between residue conformations at the endings and at the middle of the β-sheet models. Average values for T in structures VI and VIII, the twisted large models, are 13.9° and 16.8°, respectively. These values are still two times larger, at least, than interstrand twist in the corresponding flat models. Interstrand twisting in the fully relaxed twisted large models is evident in Figure 2b. According to these results, strand lengthening does not change our observations regarding the development of intra- and interstrand twisting in the flat and twisted models.

Table 5. Energetic Stability (ΔE in kcal/mol) of Twisted β-Sheets with Respect to the Corresponding Flat Ones

	antiparallel		parallel	
	small	large	small	large
ΔE	0.3	0.7	0.1	2.1

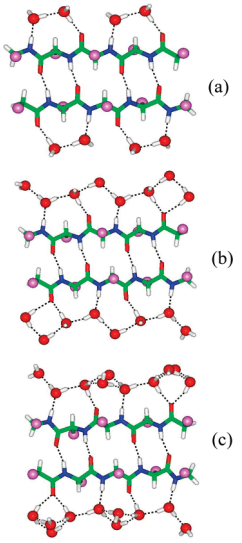

Figure 3. Small antiparallel flat β-sheet model microsolvated with (a) 8 , (b) 16, and (c) 20 water molecules. In the small antiparallel twisted β-sheet model the relative orientation of water molecules respect to the backbone is the same as depicted here. For the color code see caption of Figure 1. For clarity methyl groups are represented as pale magenta balls. Dotted lines indicate hbs.

The relative stability of twisted β-sheets with respect to the flat ones, calculated as $\Delta E = E_{twist} - E_{flat}$, where E_{twist} is the total energy of twisted sheets and E_{flat} the total energy of the corresponding flat ones, is listed in Table 5. These ΔE values are small in all the cases, indicating that both flat and twisted conformations can be adopted by parallel and antiparallel polyalanine β-sheets, though flat conformations may be preferred over twisted ones in vacuum. The stability trend may change if van der Waals interactions are taken into account. However it is expected a minimal alteration of such a trend as the spatial distribution of atoms in the flat and in the corresponding twisted conformation is very similar, hence similar van der Waals contributions to the stability of both flat and twisted structures.

Next the effect of hydration on the structure and the relative stability of β-sheets is investigated fully optimizing the geometry of flat and twisted β-sheets in which 8, 16, and 20 water molecules were adsorbed along the backbone. Only the small antiparallel β-sheet models, structures I and II, were microsolvated. Water

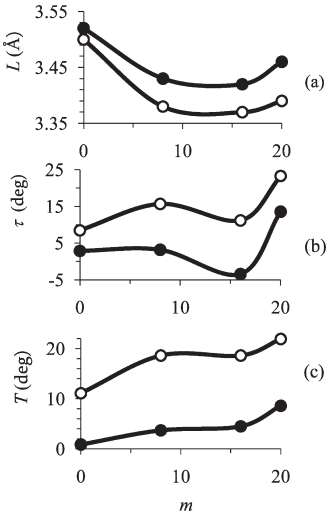

Figure 4. Change in the geometric parameters for the central residue with respect to the number of water molecules, m, in microsolvated antiparallel β-sheet models: (a) change in the rise, (b) change in the intrastrand twist, and (c) change in the interstrand twist. Closed circles stand for flat β-sheets. Open circles stand for twisted β-sheets. Solid lines are added for guiding the eye.

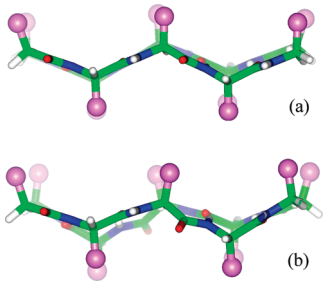

Figure 5. Flat to twist transition upon microsolvation with 20 water molecules: (a) flat conformation hydrated with 8/16 water molecules and (b) flat conformation hydrated with 20 water molecules. For the color code see caption of Figure 1. For clarity methyl groups are represented as pale magenta balls, and water molecules are not depicted.

molecules were absorbed such that an uninterrupted network of hbs, if possible, was formed along water molecules. The purpose of the latter is to investigate the effect of water−water hb cooperativity on the twist of β-sheets. It is expected that hydrated models constructed in such way resemble better a fully solvated peptide. A full scan of all possible water molecule orientations is beyond scope of the present work.

Among the several water molecule orientations examined, those shown in Figure 3 are the most stabilizing ones, and their orientations are equivalent in both flat and twisted β-sheets. Focusing on the geometric parameters for the central residues to avoid ending effects (see discussion above), it is found that L is systematically smaller than the corresponding values for vacuum structures (Figure 4a). The rise is reduced, on average, 2% and 3% due to hydration, i.e., hydration applies further compressive strain along the strands. Intrastrand twist increases as a response to hydration (Figure 4b). In particular average values for τ in the microsolvated structures with 20 water molecules are significantly larger (around three to four times larger) than the corresponding

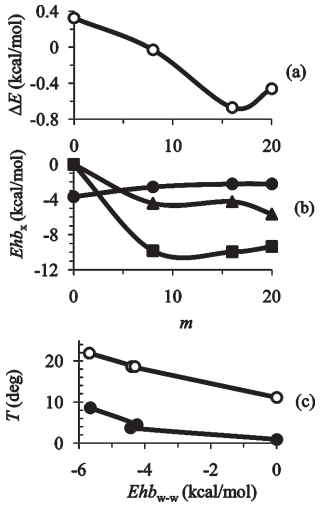

Figure 6. (a) Relative stability of the twisted antiparallel β-sheet respect to the flat one as the number of water molecules microsolvating the system, m, is increased. (b) Change in the hb strength in the microsolvated antiparallel β-sheets with respect to m. Circles stand for strand−strand hbs, $E\text{hb}_{s-s}$. Triangles stand for water−water hbs, $E\text{hb}_{w-w}$. Squares stand for strand-water hb, $E\text{hb}_{w-s}$. (c) Change in the interstrand twist, T, of microsolvated antiparallel β-sheets with respect to the strength of $E\text{hb}_{w-w}$, solid circles stand for the flat β-sheet and open circles for the twisted one. Solid lines connecting the points are added solely to guide the eye.

τ values for the structures in vacuum. The average τ value for structure I (the flat model) hydrated with 20 water molecules is even larger than the average τ value for the nonhydrated structure II (the twisted model), suggesting that the former structure is not longer flat. Interstrand twist also increases in hydrated structures (Figure 4c). The T value in the flat model (structure I) microsolvated with 20 water molecules is significantly larger, around 9 times larger, than the corresponding T value for the flat model (structure I) in vacuum, thus illustrating that the flat β-sheet transformed into a twisted one upon hydration. The latter is corroborated by the side view of the fully relaxed hydrated structures corresponding to the flat model (Figure 5). It is evident that the structure microsolvated with 20 water molecules is not longer flat.

Regarding the relative stability of twisted structures with respect to the flat ones upon hydration, it is shown in Figure 6a that ΔE becomes negative for hydrated structures. This trend indicates that twisted conformations are slightly favored over flat ones upon hydration. For the β-sheets hydrated with 20 water molecules, the stability of twisted respect to flat is reduced owing to the fact that the latter is not longer flat but twisted, i.e., the structure of the reference state changes and gets similar to that of the twisted state. Obviously the discussion presented above with respect to the influence of van der Waals interactions on the energy trend also applies here.

To get insight into why the β-sheet models microsolvated with 20 water molecules largely change their intra- and interstrand twist, hydrogen-bonding contributions to the total association energy have been analyzed. These contributions are the strand−strand hb contribution calculated as $E\text{hb}_{s-s} = [E_{s-s}(\text{bare}) - 2E_{FES}]/\text{hb}_{s-s}$, where $E_{s-s}(\text{bare})$ is the total energy of the bare β-sheet in the geometry corresponding to the hydrated one, E_{FES} is the energy of the fully relaxed strand forming the β-sheet, and

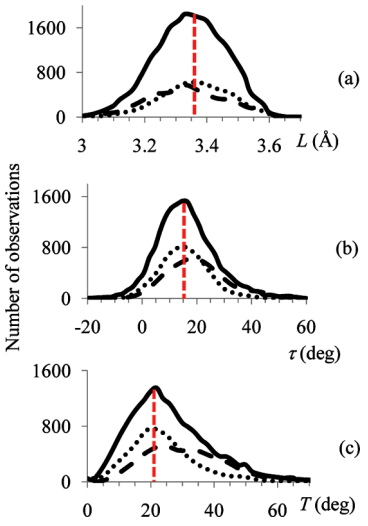

Figure 7. Distribution of values for the local geometric parameters of residues in antiparalel β-sheet motifs in protein crystals: (a) rise, L, (b) intrastrand twist, τ, and (c) interstrand twist, T. Solid line stands for all residues. Dotted lines stand for residues with no contact with water. Dashed lines stand for residues in contact with water. Dashed vertical lines mark the position of the peak for the distribution for all residues. For comparison purposes the distribution values for residues in contact with water are scaled five times.

hb_{s-s} is the number of −N−H··O hbs between strands. The water−water hb contribution calculated as $Ehb_{w-w} = [E_{hy} - mE_w]/hb_{w-w}$, where E_{hy} is the total energy of the hydrating water molecules in the geometry corresponding to the hydrated system but in the absence of the β-sheet, E_w is the total energy of a fully relaxed water molecule, m is the number of water molecules hydrating the β-sheet, and hb_{w-w} the number of −OH··OH− hbs. And the strand−water hb contribution calculated as $Ehb_{w-s} = [E_{sheet} - E_{s-s}(bare) - E_{hy}]/hb_{w-s}$, where E_{sheet} is the total energy of the hydrated β-sheet and hb_{w-s} is the number of −NH···OH− and −CO···OH− hbs. The strength of these hbs with respect the number of hydrated water molecules is depicted in Figure 6b. Only hbs of the bare/hydrated structure I are considered in plot of Figure 6b because the difference in the strength with respect to the corresponding hbs in the bare/hydrated structure II is small, around 0.2 kcal/mol or less. According to Figure 6b, Ehb_{w-s} is significantly stronger than Ehb_{w-w} and Ehb_{s-s}, being the latter the weakest one. In the bare structure the strength of these strand−strand hbs is −3.7 kcal/mol, which is in agreement with values reported in the literature.[13,38] This strength is reduced up to −2.2 kcal/mol upon hydration. For β-sheets hydrated with 20 water molecules Ehb_{w-w} becomes ∼1.4 kcal/mol stronger than that of Ehb_{w-w} in structures hydrated with 8 and 16 water molecules. On the contrary Ehb_{w-s} becomes weak by ∼0.6 kcal/mol. Thus the large twist for the β-sheets hydrated with 20 water molecules seems to be related to noticeable changes in Ehb_{w-w} and Ehb_{w-s}. Correlating the strength of the different hbs with the interstrand twist, it is found that T increases as Ehb_{w-w} become stronger (Figure 6c). Such trend thus indicates that a flat to a twist transition is primarily driven by the strengthening of Ehb_{w-w}. Strands adjust its twist to favor stronger water−water interactions even that it does weaken Ehb_{w-s} and Ehb_{s-s}.

Real β-sheets are usually twisted in globular proteins. Then it is desirable to know how the structural parameters predicted by DFT-PBE compare with that of real β-sheets in protein crystals. This comparison gives information on the influence of hydration and strand aminoacid composition on the tendency to twist. An extensive set of protein structures derived from X-ray crystallography is analyzed to obtain the corresponding distribution of values for the local geometric parameters (L_i, τ_i, and T_i). The criteria to determine if a residue belongs to a β-sheet are described in the Method Section. Only results for residues in antiparallel β-sheet motifs are presented, however, similar results were found for residues in parallel β-sheets. It is found that 14% of the residues in the investigated set are in β-sheet like motifs, 10% in antiparallel, and 4% in parallel conformation. The corresponding (L_i, τ_i, T_i) distributions of values for residues in antiparallel β-sheets are shown in Figure 7. The values for L, τ, and T corresponding to the peak of the distributions are $L \approx 3.35$ Å, $\tau \approx 15°$, and $T \approx 22°$. These values are in good agreement with those predicted by DFT-PBE for antiparallel β-sheets, particularly for microsolvated ones. Considering that the set of analyzed residues in β-sheet conformation contains only 8% of alanine, the good agreement between predicted and observed values for τ and T indicates that strand amino acid composition has little influence on inter- and intrastrand twist in real β-sheets. To investigate the effect of hydration on the twist of β-sheet motifs in protein crystals, the (L_i, τ_i, T_i) distribution of values has been obtained considering: (i) only residues in contact with water molecules (hydrated) in the set of studied proteins and (ii) only residues with no contact at all with water (nonhydrated). A residue was considered to be in contact with water if the distance between the N or O atoms of the peptide unit and the O atoms of water was less than 3 Å. The number of hydrated residues forming β-sheets was found to be significantly smaller than nonhydrated ones forming β-sheets. For comparison purposes the distribution of values for residues in contact with water is scaled five times. The (L_i, τ_i, T_i) distribution of values (Figure 7) shows a tendency that agrees with DFT results. The peak of the L distribution for hydrated residues is shifted toward smaller values of L with respect to the corresponding peak for nonhydrated ones (Figure 7a). Thus hydration applies compression along the backbone chain, as predicted by DFT-PBE. The peak of the τ distribution for the hydrated residues is shifted to larger values with respect to the peak for nonhydrated ones (Figure 7b). The latter indicates that hydration induces larger intrastrand twist as predicted by DFT-PBE. Also the trend observed for the distribution of T values is in agreement with the DFT-PBE results. The position of the peaks of the distribution indicates that hydration favors a larger interstrand twist (Figure 7c).

4. DISCUSSION

To discuss the sufficiency of the models here studied, average standard geometrical parameters (ϕ, ψ dihedral angles and interstrand hydrogen-bonding distances) for the optimized models are compared to experimental values from the literature. The reported (ϕ, ψ) mean values for alanine in antiparallel β-sheet motifs are $\phi_{exp} = -130.2 \pm 21.4°$ and $\psi_{exp} = 143.8 \pm 14.6°$.[39] Average ($\phi$, ψ) values for our bare antiparallel β-sheet models are (−144.7°, 151.6°), (−136.9°, 150.4°), (−149.3°, 153.8°), and (−139.2°, 153.3°) for models I, II, V, and VI, respectively. The corresponding (ϕ, ψ) average values for the flat models hydrated with 8, 16, and 20 water molecules are (−132.2°, 137.0°), (−136.0°, 131.2°), and (−128.2°, 149.0°), respectively. And for the corresponding twisted hydrated models are (−118.2°,

136.8°), (−120.4°, 132.9°), and (−114.1°, 147.6°). All these theoretical values fall inside the range of the standard deviation for (ϕ_{exp}, ψ_{exp}). The same is found for the parallel β-sheet models. The reported (ϕ, ψ) mean values for alanine in parallel β-sheet motifs are $\phi_{exp} = -122.0 \pm 22.0°$ and $\psi_{exp} = 136.6 \pm 16.8°$.[39] The average ($\phi$, ψ) values for the parallel β-sheet models investigated here are (−135.5°, 137.7°), (−127.4°, 140.7°), (−135.2°, 137.6°), and (−131.4°, 144.3°) for the models III, IV, VII, and VIII, respectively. Furthermore the average N−H···O hydrogen-bonded distances for the bare (2.0 Å) and the hydrated (1.9 Å) β-sheet models are in agreement with theoretical values reported in the literature.[15,17,38,40] Moreover these values also fall in the range of the standard deviation for the corresponding values in crystal structures in proteins (1.96 ± 0.16 Å for antiparallel and 1.97 ± 0.15 Å in parallel β-sheets).[41] These results give us confidence in the models used for describing β-sheet conformations.

Despite the compelling evidence indicating that β-sheets adopt both flat and twisted conformations, there is no consensus on the reasons underlying such behavior. Several studies have pointed out that isolated strands have an intrinsic tendency to twist.[7,8,12,18,20] Indeed the structure connected to the minimum in the DFT-PBE potential energy surface for isolated polyalanine in extended conformation is left-hand twisted by 3° (see, e.g., Figure 2 in ref 33).[33,34] However the latter value is around three times smaller than a typical intrastrand twist in a real β-sheet (see, e.g., Figure 7b). Moreover if the observed twist in real β-sheets is due to the intrinsic intrastrand twist of isolated strands, then one should explain why some β-sheets adopt flat conformations. Thus effects not connected to the intrinsic asymmetry of the minimum of the potential energy surface must be considered to explain the large intra- and interstrand twist in real β-sheets. In this work it is shown that strands in β-sheets are under compressive strain. According to ref 33, polyalanine backbone tends toward left-hand twist under compressive strain. Here it is found that β-sheets in which all residues locally twist to the left as response to compressive strain develop a right-handed interstrand twist. In flat β-sheets, however, residues are not as compressed as in twisted β-sheets and develop both left- and right-handed local intrastrand twist. The latter leads to an average intrastrand twist that is not large enough to force a noticeable interstrand twist in vacuum. Likely, local interstrand repulsive contacts prevent that all residues in flat sheets twist to the left upon interstrand hydrogen bonding, i.e., the response of the backbone to the compressive strain applied by hydrogen bonding is frustrated by local interstrand contacts. Microsolvation applies further compressive strain along strands favoring twisting. Residues in hydrated flat sheets adjust the sense of its intrastrand twist as a response to the extra compressive strain. Therefore flat sheets transform to twisted ones upon hydration. Compressive strain arising from microsolvation is likely exerted by water−water hydrogen bonding. In a network of aligned hbs the interaction is strengthened, and the hydrogen-bonding distance gets shorter due to a cooperative effect. The water−water hbs formed upon hydration with eight water molecules promote a reduction between 2% and 3% in the rise of the residues (see Figure 4a) and increase their interstrand twist by more than 60% with respect to residues in the bare β-sheets. Increasing the number of hydrating water molecules up to 16 does not change the water−water hydrogen-bonding strength (Figure 6b), therefore the rise and the interstrand twist do not change significantly (Figure 4). A further increment in the number of hydrating water molecules up to 20 strengthens the water−water hydrogen bonding around 30%. Such an increment in the water−water strength, however, does not longer compress the residues; probably intra- and/or interstrand contacts prevent it. Therefore residues release the extra strain with a strong change in their intrastrand twist followed by a noticeable change in the interstrand twist. Thus in microsolvated β-sheets, strands tend to further reduce its rise and/or to change its twist to favor the development of an optimal network of hbs, i.e., to maximize Ehb_{w-w}, along the water molecules.

The analysis of the geometry of residues in real β-sheet motifs from an extended set of protein crystals supports the tendencies predicted by our calculations. Moreover, predicted conformations correspond to alanine, and the observed ones to all residues except glycine and proline, hence twisting is independent of the amino acid composition of the strands. Furthermore, the agreement between the predicted and observed twist in real β-sheet motifs gives confidence to the results obtained with DFT-PBE.

5. CONCLUSIONS

In conclusion the results presented in this work indicate that twisted and flat structures are intrinsic conformations of both parallel and antiparallel β-sheets. It is shown that twisting primarily results as a response of the backbone to compressive strain applied by interstrand interactions and hydration. Moreover it is shown that the strengthening of water−water hydrogen bonding along the solvation shell of β-sheets promotes a flat to twist transition. The good agreement between predicted and observed conformations of residues in β-sheet motifs in protein crystals corroborates the effect of hydration on the twist of β-sheets here described. Therefore the models here investigated are realistic, hence useful for elucidating more accurate atomistic models, for e.g., amyloid-like fibrils.

AUTHOR INFORMATION

Corresponding Author
*E-mail: iret@xanum.uam.mx.

ACKNOWLEDGMENT

The author thanks the Laboratorio de Visualización y Cómputo en Paralelo at UAM-Iztapalapa.

REFERENCES

(1) Lehninger, A. L.; Nelson, D. L.; Cox, M. M. Principles of Biochemistry, 2nd ed.; Worth: New York, 1993; Chapter 4, pp 123.
(2) Nelson, R.; Sawaya, M. R.; Balbirnie, M.; Madsen, A. Ø.; Riekel, C.; Grothe, R.; Eisenberg, D. *Nature* **2005**, *435*, 773–778.
(3) Sawaya, M. R.; Sambashivan, S.; Nelson, R.; Ivanova, M. I.; Sievers, S. A.; Apostol, M. I.; Thompson, M. J.; Balbirnie, M.; Wiltzius, J. J. W.; McFarlane, H. T.; Madsen, A. Ø.; Reikel, C.; Eisenberg, D. *Nature* **2007**, *447*, 453–457.
(4) Sunde, M.; Serpell, L. C.; Bartlam, M.; Fraser, P. E.; Pepys, M. B.; Blake, C. C. F. *J. Mol. Biol.* **1997**, *273*, 729–739.
(5) Nelson, R.; Eisenberg, D. *Adv. Protein Chem.* **2006**, *73*, 235–282.
(6) Dobson, C. M. *Nature* **2005**, *435*, 747–749.
(7) Maccallum, P. H.; Poet, R.; Milner-White, E. J. *J. Mol. Biol.* **1995**, *248*, 374–384.
(8) Yang, A. S.; Honig, B. *J. Mol. Biol.* **1995**, *252*, 366–376.
(9) Weatherford, D. W.; Salemme, F. R. *Proc. Natl. Acad. Sci. U.S.A.* **1979**, *76*, 19–23.
(10) Chou, K. C.; Némethy, G.; Scheraga, H. A. *J. Mol. Biol.* **1983**, *168*, 389–407.

(11) Wang, L; O'Connell, T.; Tropsha, A.; Hermans, J. *J. Mol. Biol.* **1996**, *262*, 283–293.
(12) Shamovsky, I. L.; Ross, G. M.; Riopelle, R. J. *J. Phys. Chem. B* **2000**, *104*, 11296–11307.
(13) Rossmeisl, J.; Nørskov, J. K.; Jacobsen, K. W. *J. Am. Chem. Soc.* **2004**, *126*, 13140–13143.
(14) Zhao, Y.-L.; Wu, Y.-D. *J. Am. Chem. Soc.* **2002**, *124*, 1570–1571.
(15) Scheiner, S. *J. Phys. Chem. B* **2006**, *110*, 18670–18679.
(16) Perczel, A.; Gáspári, Z.; Csizmadia, I. G. *J. Comput. Chem.* **2005**, *26*, 1155–1168.
(17) Viswanathan, R.; Asensio, A.; Dannenberg, J. J. *J. Phys. Chem. A* **2004**, *108*, 9205–9212.
(18) Chothia, C. *J. Mol. Biol.* **1973**, *75*, 295–302.
(19) Salemme, F. R. *Prog. Biophys. Mol. Biol.* **1983**, *42*, 95–133.
(20) Ho, B. K.; Curmi, P. M. G. *J. Mol. Biol.* **2002**, *317*, 291–308.
(21) Periole, X.; Rampioni, A.; Vendruscolo, M.; Mark, A. E. *J. Phys. Chem. B* **2009**, *113*, 1728–1737.
(22) Esposito, L.; Pedone, C.; Vitagliano, L. *Proc. Natl. Acad. Sci. U.S. A.* **2006**, *103*, 11533–11538.
(23) Plumley, J. A.; Dannenberg, J. J. *J. Am. Chem. Soc.* **2010**, *132*, 1758–1759.
(24) Perdew, J.; Burke, K.; Ernzerhof, M. *Phys. Rev. Lett.* **1996**, *77*, 3865–3868.
(25) Ireta, J.; Neugebauer, J.; Scheffler, M. *J. Phys. Chem. A* **2004**, *108*, 5692–5698.
(26) Troullier, N.; Martins, J. L. *Phys. Rev. B* **1991**, *43*, 1993–2006.
(27) Fuchs, M.; Scheffler, M. *Comput. Phys. Commun.* **1999**, *119*, 67–98.
(28) ((a)) Gonze, X.; Beuken, J. M.; Caracas, R.; Detraux, F.; Fuchs, M.; Rignanese, G. M.; Sindic, L.; Verstraete, M.; Zera, G.; Jollet, F.; Torrent, M.; Roy, A.; Ghosez, P.; Raty, J. Y.; Allan, D. C. *Comput. Mater. Sci.* **2002**, *25*, 478–492. ((b)) Gonze, X.; Rignanese, G. M.; Verstraete, M.; Beuken, J. M.; Pouillon, Y.; Caracas, R.; Jollet, F.; Torrent, M.; Zerah, G.; Mikami, M.; Ghosez, P.; Veithen, M.; Raty, J. Y.; Olevano, V.; Bruneval, F.; Reining, L.; Godby, R.; Onida, G.; Hamann, D. R.; Allan, D. C. *Z. Kristallogr.* **2005**, *220*, 558–562.
(29) Torrent, M.; Jollet, F.; Bottin, F.; Zerah, G.; Gonze, X. *Comput. Mater. Sci.* **2008**, *42*, 337–351.
(30) Kearsley, S. K. *Acta Cryst. A* **1989**, *45*, 208–210.
(31) Quine, J. R. *J. Mol. Struct. (THEOCHEM)* **1999**, *460*, 53–66.
(32) Kneller, G. R.; Calligari, P. *Acta Crystallogr., Sect. D: Biol. Crystallogr.* **2006**, *62*, 302–311.
(33) Ireta, J. ; Scheffler, M. *J. Chem. Phys.* **2009**, *131*, art-085104.
(34) Penev, E.; Ireta, J.; Shea, J.-E. *J. Phys. Chem. B* **2008**, *112*, 6872–6877.
(35) Ireta, J.; Neugebauer, J.; Scheffler, M.; Rojo, A.; Galván, M. *J. Am. Chem. Soc.* **2005**, *127*, 17241–17244.
(36) Calligari, P. A.; Kneller, G. R.; Giansanti, A.; Ascenzi, P.; Porrello, A.; Bocedi, A. *Biophys. Chem.* **2009**, *141*, 117–123.
(37) Berman, H. M.; Westbrook, J.; Feng, Z.; Gilliland, G.; Bhat, T. N.; Weissig, H.; Shindyalov, I. N.; Bourne, P. E. *Nucleic Acids Res.* **2000**, *28*, 235–242.
(38) Plumley, J. A.; Tsai, M. I-H.; Dannenberg, J. J. *J. Phys. Chem. B* **2011**, *115*, 1562–1570.
(39) Hovmöller, S.; Zhou, T.; Ohlson, T *Acta Crystallogr., Sect. D: Biol. Crystallogr.* **2002**, *58*, 768–776.
(40) Rossmeisl, J.; Hinnemann, B.; Jacobsen, K. W.; Nørskov, J. K. *J. Chem. Phys.* **2003**, *118*, 9783–9794.
(41) Baker, E. N.; Hubbard, R. E. *Prog. Biophys. Mol. Biol.* **1984**, *44*, 97–179.